Crystal Structure of the Glucocorticoid Receptor Ligand Binding Domain Reveals a Novel Mode of Receptor Dimerization and Coactivator Recognition

Randy K. Bledsoe,[1] Valerie G. Montana,[2,9]
Thomas B. Stanley,[1,9] Chris J. Delves,[7,9]
Christopher J. Apolito,[1] David D. McKee,[1]
Thomas G. Consler,[1] Derek J. Parks,[4]
Eugene L. Stewart,[2] Timothy M. Willson,[5]
Millard H. Lambert,[2] John T. Moore,[6]
Kenneth H. Pearce,[1,8] and H. Eric Xu[2,8,10]
[1]Gene Expression and Protein Biochemistry
[2]Computational, Analytical and Structural Sciences
[4]Nuclear Receptor Systems Research
[5]High Throughput Chemistry
[6]High Throughput Biology
Discovery Research
GlaxoSmithKline
Research Triangle Park, North Carolina 27709
[7]Gene Expression and Protein Biochemistry
Discovery Research
GlaxoSmithKline
Stevenage SG1 2NY
United Kingdom

Summary

Transcriptional regulation by the glucocorticoid receptor (GR) is mediated by hormone binding, receptor dimerization, and coactivator recruitment. Here, we report the crystal structure of the human GR ligand binding domain (LBD) bound to dexamethasone and a coactivator motif derived from the transcriptional intermediary factor 2. Despite structural similarity to other steroid receptors, the GR LBD adopts a surprising dimer configuration involving formation of an intermolecular β sheet. Functional studies demonstrate that the novel dimer interface is important for GR-mediated activation. The structure also reveals an additional charge clamp that determines the binding selectivity of a coactivator and a distinct ligand binding pocket that explains its selectivity for endogenous steroid hormones. These results establish a framework for understanding the roles of protein-hormone and protein-protein interactions in GR signaling pathways.

Introduction

The glucocorticoid receptor (GR) is a steroid hormone-activated transcriptional factor known to regulate, either directly or indirectly, target genes involved in glucose homeostasis, bone turnover, cell differentiation, lung maturation, and inflammation (Reichardt et al., 2000). Mutations in GR are associated with Cushing's syndrome, autoimmune diseases, and various cancers (Werner and Bronnegard, 1996). As such, GR is widely recognized as

a therapeutically important target. GR ligands, including dexamethasone, prednisolone, and other related corticosteroid analogs, are commonly used to treat diverse medical conditions such as asthma, allergic rhinitis, rheumatoid arthritis, and leukemia (Barnes et al., 1998). However, clinical use of oral corticosteroids is limited by a number of side effects ranging from increased bone loss and growth retardation to suppression of the hypothalamic-pituitary-adrenal axis. Discovery of a GR agonist that retains the beneficial anti-inflammatory activities without the undesired side effects is the subject of intense pharmaceutical efforts.

GR belongs to the nuclear receptor (NR) superfamily, which includes receptors for the mineralocorticoids (MR), estrogens (ER), progestins (PR), and androgens (AR), as well as receptors for peroxisome proliferators (PPARs), vitamin D (VDR), and thyroid hormones (TR). Phylogenetic analysis and sequence alignments show that GR, MR, PR, and AR form a subfamily of oxosteroid receptors that are distinct from the ER subfamily (NRNC, 1999). Like most nuclear receptors, GR is a modular protein that is organized into three major domains: an N-terminal activation function-1 domain (AF-1), a central DNA binding domain (DBD), and a C-terminal ligand binding domain (LBD). In addition to its role in ligand recognition, the LBD contains a ligand-dependent activation function (AF-2) that is tightly regulated by hormone binding.

Within the context of the full-length receptor, both the AF-1 function and the DNA binding activity of GR are dependent on hormone binding. In the absence of ligand, GR is retained in the cytoplasm by association with chaperone proteins such as hsp90 and p23, which bind to the LBD (Pratt and Toft, 1997). The chaperone activity of the hsp90 complex has been shown to be critical for hormone binding by GR (Bresnick et al., 1989; Picard et al., 1990). Hormone binding initiates the release of chaperone proteins from GR, allowing dimerization and translocation of the receptor into the nucleus. In the nucleus, GR binds to DNA promoter elements and can either activate or repress transcription depending on the context of the target promoters. In addition, GR can also crosstalk with other transcriptional factors such as nuclear factor-κB (NF-κB) and activator protein-1 (AP-1) to repress their gene activation activities (reviewed in McKay and Cidlowski, 1999). This GR mediated repression has been postulated to be a molecular basis for the anti-inflammatory and immunosuppressive activities of glucocorticoids. Both the ligand-dependent activation and repression by GR require the intact function of the LBD.

The molecular mechanism of ligand-dependent regulation of nuclear receptors has been illustrated by crystal structures of more than a dozen NR LBDs that are either in the apo-state or bound to agonists or antagonists. (Bourguet et al., 1995; Brzozowski et al., 1997; Renaud et al., 1995; Wagner et al., 1995; Xu et al., 1999). These structures not only reveal that the LBDs fold into a canonical three-layer helical sandwich that embeds a hydrophobic pocket for ligand binding, but also highlight

[8]Correspondence: eric.xu@vai.org (H.E.X.); kenneth.h.pearce@gsk.com (K.H.P.)
[9]These authors contributed equally to this work.
[10]Present address: Laboratory of Structural Sciences, Van Andel Research Institute, 333 Bostowick NE, Grand Rapids, Michigan.

the importance of the C-terminal (AF-2) helix in ligand-dependent regulation. In the apo- or antagonist-bound receptor, the AF-2 helix is destabilized from its "active" conformation to allow the LBD to interact with corepressors such as nuclear corepressor (N-CoR) and silencing mediator for retinoid and thyroid hormone receptors (SMRT; Chen and Evans, 1995; Horlein et al., 1995). Agonist binding induces a conformational change of the AF-2 helix, stabilizing the receptor in an active conformation to facilitate its association with coactivator proteins, such as steroid receptor coactivator-1 (SRC-1) and transcriptional intermediary factor 2 (TIF2; Onate et al., 1995; Voegel et al., 1996). These coactivators contain multiple LXXLL motifs, which interact with the NR LBD (Heery et al., 1997; Le Douarin et al., 1996). Various crystal structures of receptor/coactivator peptide complexes have revealed a general mode of coactivator binding to NRs. In these structures, the coactivator LXXLL motifs adopt a two-turn α helix and both helical ends are stabilized by a "charge clamp" formed in part by a conserved acidic residue from the AF-2 helix (Darimont et al., 1998; Nolte et al., 1998; Shiau et al., 1998). However, the structural basis for the sequence specific recruitment of LXXLL motifs by different LBDs has remained ambiguous.

As DNA binding transcription factors, most NRs function as dimers. Receptor dimerization is mediated in part through the LBD. Crystal structures of the ER homodimer and two different RXR heterodimers reveal a common mode of dimerization, where the N-terminal half of helix-10 from one monomer packs against the same portion of helix-10 from the other monomer in a parallel manner (Bourguet et al., 1995; Gampe et al., 2000). The dimerization is mediated through a sequence motif of ϕ ϕK$\phi\phi$ ϕK$\phi\phi$ X ϕR$\phi\phi$ (where ϕ is a hydrophobic residue and X is any residue) that forms a coiled-coil structure in the N-terminal half of helix-10. Mutations in the ϕK$\phi\phi$ repeats in ER that abolish dimerization result in a receptor that is defective for initiating of gene transcription (Valentine et al., 2000). Like ER, GR and its related receptors AR and PR, activate transcription as homodimers and the GR LBD alone has been shown to be capable of forming a homodimer (Savory et al., 2001). The dimer interface observed in the PR LBD structure does not involve helix-10 and is significantly smaller than that seen in the RXR heterodimer or in the ER homodimer (Williams and Sigler, 1998). The physiological relevance of this PR dimer interface remains to be determined. To date, the arrangement of the GR LBD dimer has not been defined. In the full-length receptor, GR contains an additional homodimer interface on the C-terminal end of the DBD. Interestingly, a mutation (A458T) in this region of mouse GR, termed GR[dim], is defective in transcription activation but not transrepression (Reichardt et al., 1998).

Given its biological and pharmaceutical importance, there has been enormous interest in elucidating the GR LBD structure. However, these structural efforts have been hampered by the inability to obtain a purified receptor that retains ligand binding activity. In this paper, we describe expression, purification, crystallization, and structure determination of the GR LBD in complex with dexamethasone and a coactivator motif derived from the cofactor TIF2. Surprisingly, the structure reveals a novel dimer interface unlike that observed for any other nuclear receptor. Mutagenesis studies support the importance of this dimer interface in GR function. The crystal structure also reveals an unanticipated second charge clamp that is responsible for the specificity for the third TIF2 LXXLL motif, and a distinct steroid binding pocket with features that explain ligand binding and selectivity. Since GR is highly homologous to MR, AR, and PR, the structure presented here should serve as a model for understanding the roles of ligand binding, coactivator recruitment, and receptor dimerization in the signaling pathways mediated by these steroid receptors.

Results

Purification, Characterization, and Crystallization of the GR LBD

Historically, the GR LBD has been a very difficult protein to express in a recombinant form mostly due to solubility problems. We were also unsuccessful in our own attempts to express the wild-type human GR LBD at high levels even though a wide range of conditions were explored. To overcome these difficulties, we performed a sequence alignment of GR with the related steroid receptors PR and AR, which have been previously expressed and purified from E. coli (Matias et al., 2000; Sack et al., 2001; Williams and Sigler, 1998). This analysis was initiated to identify residues that are hydrophobic in GR but hydrophilic in PR and AR as they might contribute to solubility or aggregation problems. We also built a structural model for GR by using its homology to the PR LBD to explore the molecular basis of the poor behavior of the GR protein and to prioritize residues for systematic mutagenesis. Strikingly, we found that a single phenylalanine to serine mutation in helix 5 (F602S) significantly improved E. coli expression of a soluble GR LBD (residues 521–777) in the presence of dexamethasone (Figure 1A). This point mutant LBD was purified to homogeneity for biochemical and structural studies described below.

To assess the functional activity of the purified GR LBD, we used a fluorescence polarization assay to test the binding of a fluorescently labeled dexamethasone derivative to the receptor. In this experiment, we attempted to remove the excess dexamethasone carried over from purification by extensive dialysis. Figure 1B shows that this dialyzed GR LBD exhibits dose-dependent saturable binding to the fluorescent dexamethasone derivative with an apparent affinity of 60 nM. Addition of excess unlabeled dexamethasone completely inhibited the binding signal of the labeled dexamethasone derivative.

Dexamethasone is a potent agonist that promotes the binding of coactivators to GR (Ding et al., 1998). To test the ability of the dexamethasone-bound GR LBD to recruit coactivators, we used surface plasmon resonance to measure the interaction of the receptor with a peptide containing the third LXXLL motif from TIF2 (Voegel et al., 1998). TIF2 is the human homolog of the mouse GR interacting protein 1 (GRIP1) and its third LXXLL motif has been shown to be preferred by GR (Ding et al., 1998). Figure 1C shows that addition of a 5-fold excess of dexamethasone enhances the binding
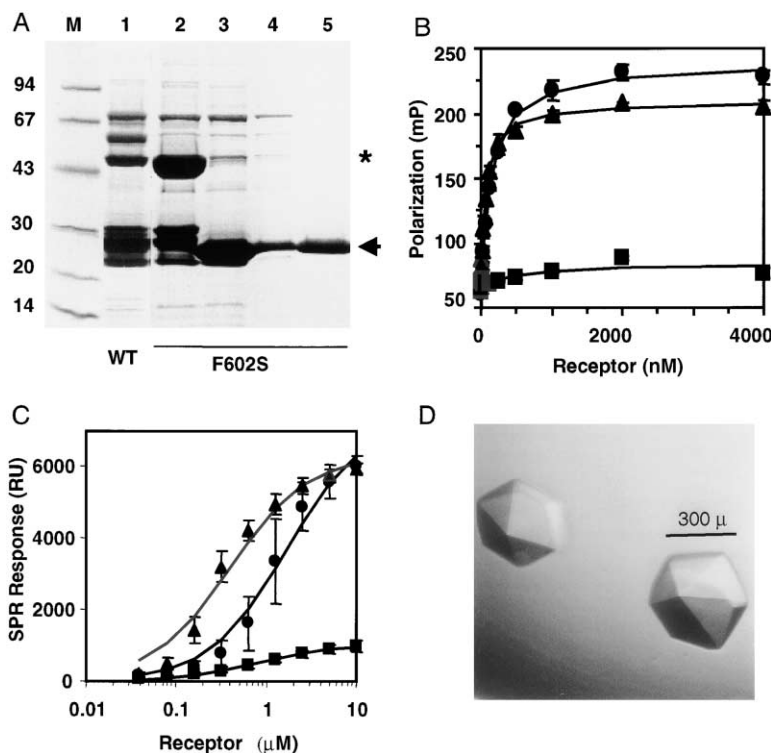
Figure 1. Purification and Characterization of the GR LBD

(A) Comparison of the protein expression of wild-type GR (lane 1) and the F602S GR (lane 2) in the presence of 10 μM dexamethasone. The proteins shown are the soluble fractions eluted from the Ni^{2+} column. Lanes 3–5 show the purification of the F602S GR LBD (lane 3, the sample after thrombin digestion; lane 4, the Ni^{2+} column flow through of the thrombin-digested sample; lane 5, the final purified protein. The molecular weight markers are shown in lane M and the 6 × HisGST-fused and cleaved GR LBD are indicated with a star and an arrow, respectively.

(B) Binding of dexamethasone to the purified GR F602S proteins as measured by fluorescence polarization assays (circles: GST-GR LBD; triangles: GR LBD; and squares: GR LBD in the presence of 100 μM unlabeled dexamethasone).

(C) Ligand-dependent binding of TIF2 coactivator motif to GST-GR LBD in the presence of a 5-fold excess of dexamethasone (triangles), RU486 (squares), and no compound (circles) was measured by surface plasmon resonance.

(D) Crystals of the GR/Dex/TIF2 complex.

of the TIF2 coactivator peptide to the purified and dialyzed GR LBD. In contrast, addition of a 5-fold excess of RU486, a known GR antagonist, inhibited the binding of the receptor to the TIF2 peptide. These results demonstrate that the purified GR LBD is able to bind either an agonist or an antagonist in the absence of the hsp90 chaperone. Importantly, the ligand-mediated association of the TIF2 peptide to the purified GR correlates with the agonist and antagonist properties of dexamethasone and RU486. Based on these results, a ternary complex of the purified GR LBD bound with dexamethasone and the TIF2 peptide was prepared and crystallized (Figure 1D).

Structure of the GR/Dexamethasone/TIF2 Complex

The GR/dexamethasone/TIF2 complex was crystallized in the P61 space group with two complexes in each asymmetric unit. Data sets were collected from two independent crystals to 2.8 Å and 2.5 Å, respectively. We determined both structures by the molecular replacement method using a GR model built from the PR LBD structure (see Experimental Procedures). The electron density map calculated with the molecular replacement solutions showed clear tracing for two GR LBD monomers (residues 523–777), two bound molecules of dexamethasone, and the LXXLL motifs of the two TIF2 peptides. The statistics of data sets and the refined structures are summarized in Table 1.

In the crystals, each GR LBD is bound to a molecule of dexamethasone and a TIF2 coactivator peptide (Figure 2A). The structure of the GR LBD contains 11 α helices and 4 small β strands that fold into a three-layer helical domain with an overall organization closely

resembling the structures of PR and AR (Matias et al., 2000; Sack et al., 2001; Williams and Sigler, 1998). Helices 1 and 3 form one side of a helical sandwich whereas helices 7 and 10 form the other side. The middle layer of helices (helices 4, 5, 8, and 9) are present in the top half of the protein but are absent in the bottom half of the protein. This arrangement of helices creates a cavity in the bottom half of the GR LBD where the dexamethasone molecule is bound. The AF-2 helix, which plays an essential function in ligand-dependent activation, adopts the so-called "agonist bound" conformation where it packs against helices 3, 4, and 10 as an integrated part

Table 1. Statistics of Crystallographic Data and Structures

Crystals	1	2
X-ray Source	Rigaku-200	APS-17BM
space group	P6₁	P6₁
resolution (Å)	20.0–2.8	50.0–2.5
unique reflections	18,923	27,095
completeness (%)	99.7	99.4
I/σ (last shell)	25.7 (2.3)	35.9 (2.5)
R_{sym}[a] (%)	8.5	8.2
Refinement statistics		
R factor[b] (%)	25.4	23.7
R free (%)	30.8	26.7
rmsd bond lengths (Å)	0.015	0.007
rmsd bond angles (degrees)	1.800	1.500
total non-hydrogen atoms	4502	4845

rmsd is the root mean square deviation from ideal geometry.
[a] $R_{sym} = \Sigma \mid Iavg - Ii \mid / \Sigma \; Ii$
[b] $R_{factor} = \Sigma \mid F_P - F_{Pcalc} \mid / \Sigma F_P$, where F_P and F_{pcalc} are observed and calculated structure factors, R_{free} was calculated from a randomly chosen 10% of reflections excluded from refinement and R_{factor} was calculated for the remaining 90% of relfections.
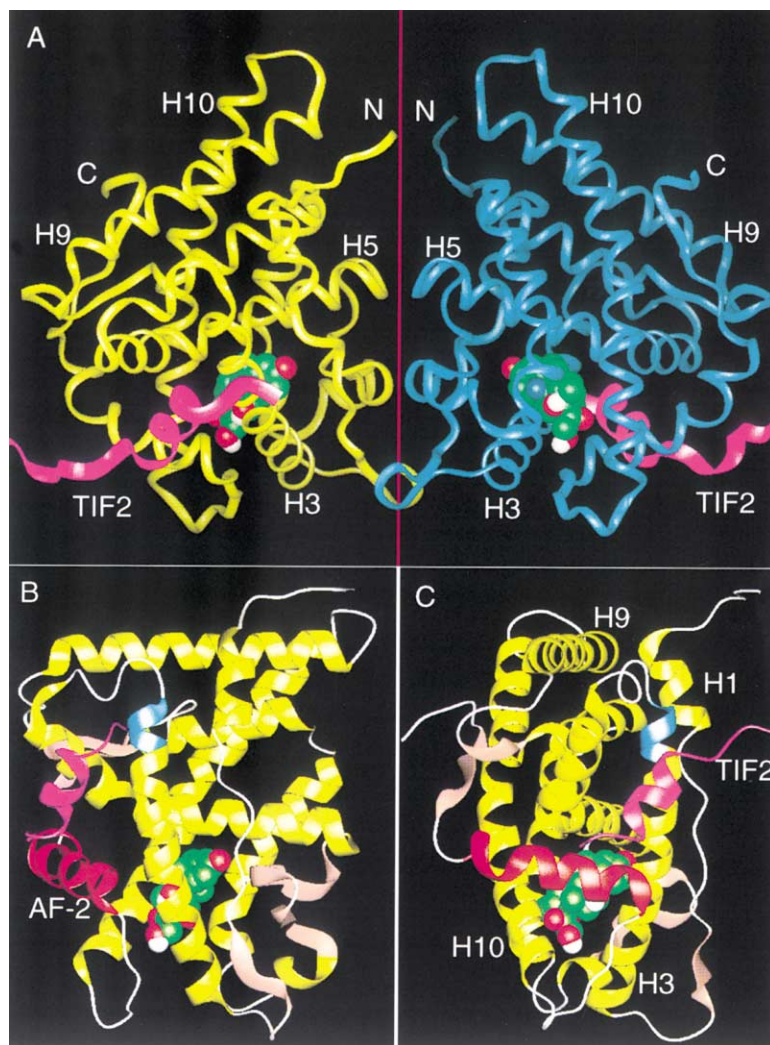
Figure 2. Structure of the GR/Dex/TIF2 Complex

(A) Overall arrangement of the GR LBD dimer. The two LBDs are shown in yellow and blue worms; the two TIF2 peptides are in purple ribbon; and the two dexamethasone molecules are in space-filling representation with carbon, oxygen, and hydrogen colored in green, red, and white, respectively. The C2 symmetry axis is shown in red.

(B and C) Two 90-degree views of the GR/Dex/TIF2 monomer complex, where helices are colored in yellow and β strands are in gold. The AF-2 helix is in red and the lysine residue from helix 3 that forms the charge clamp is in blue. The TIF2 peptides are shown in purple.

of the domain structure. Following the AF-2 helix is an extended strand that forms a conserved β sheet with a β strand between helices 8 and 9. This C-terminal β strand also appears to play an important role in receptor activation by stabilizing the AF-2 helix in the active conformation. Deletion of the last few residues that form the β strand resulted in an inactive receptor (Zhang et al., 1996).

The GR Dimer Interface

Strikingly, the two GR LBD monomers in each asymmetric unit are arranged in a unique dimer configuration. Unlike the asymmetric arrangement of the PPARγ/RXR heterodimer structures (Gampe et al., 2000), the two GR monomers show a C2 symmetric packing arrangement in which either LBD can be superimposed on the other by rotating 180 degrees around the 2-fold axis (Figure 2A). Formation of the dimer buries 623 Å^2 of solvent accessible surface in the dimer interface, which is also stabilized by a series of hydrophobic and hydrogen bond interactions (Figure 3A). The central hydrophobic interface is made up of reciprocal interactions between residues P625 and I628 in the β turn of strands 3 and 4 (Figure 3B). Surrounding this core hydrophobic interface is an extensive network of hydrogen bonds mediated by

the extended strand between helices 1 and 3 (residues 547–551) and the last residue of helix 5 (Q615). In particular, residues 547–551 from each LBD, resembling two anti-parallel β strands, are in excellent geometry to form four hydrogen bonds (Figure 3C). These hydrogen bonds may also play a key role in stabilizing the GR dimer configuration.

To confirm the presence of dimeric GR LBD in solution, we analyzed the distribution of monomers and dimers in the GR population by equilibrium analytical ultracentrifugation. In the presence of both dexamethasone and the TIF2 peptide, a clear monomer-dimer equilibrium was observed with an apparent dimerization affinity (Kd) of 1.5 μM (Figure 4A). We further confirmed the presence of the GR dimer in solution by dynamic light scattering. In this experiment, the PPARγ/RXR heterodimer was used as a positive control with a measured hydrodynamic diameter of 84 Å, which is consistent with the actual size of the heterodimer observed in PPARγ/RXR crystal structure (Gampe et al., 2000). The hydrodynamic diameter of the GR LBD complex was measured to be 82 Å, which is also closely correlated with the side to side distance of 83–88 Å observed in the GR dimer structure.

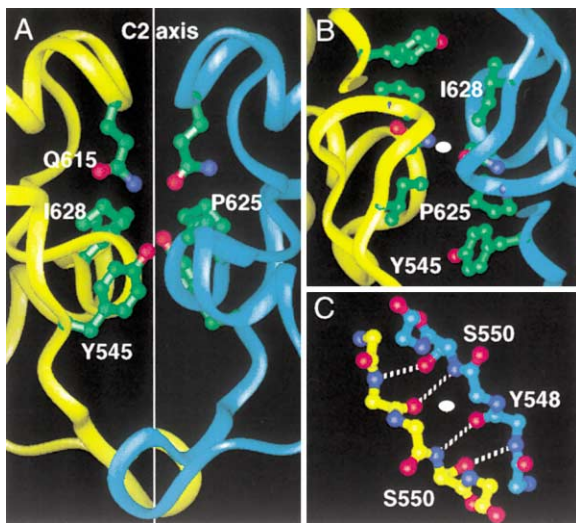Since P625 and I628 make up the core hydrophobic

Figure 3. Characterization of the GR Dimer Interface

(A) The GR dimer interface showing the key residues and the pseudo β strands (bottom). The I628 and P625 are labeled for the two LBDs (colored in yellow and blue, respectively).

(B) The core hydrophobic interactions between the two GR LBDs. The I628 and P625 are both labeled for the blue monomer.

(C) The hydrogen bond network between the pseudo β strands.

dimer interface, these residues were mutated to alanine within the context of the F602S mutant to test their role in LBD-LBD dimerization. The P625A/F602S LBD protein was insoluble in *E. coli* and was not useful for biochemical studies. However, the I628A/F602S GR LBD is nearly as soluble as the F602S LBD (Figure 4B) and was purified to homogeneity for in vitro characterization (lane 7 in Figure 4B). As measured by analytical ultra-centrifugation, the I628A/F602S mutant LBD showed a 10-fold decrease in dimerization affinity as compared to the F602S GR LBD (Figure 4A). These results demonstrate that the GR LBD forms a dimer in solution and the interface observed in the crystal structure is required for effective dimerization.

Functional Analysis of GR Dimer Interface

To test the functional significance of the dimer interface observed in the GR LBD, we mutated P625 and I628 to alanine within the context of the full-length receptor. We characterized these mutants in a transient transfection assay using a reporter driven by the MMTV promoter. In the presence of dexamethasone, the wild-type and the F602S mutant receptors induced 46.0-fold and 46.8-fold activation, respectively (Figure 4C). The P625A and I628A mutant proteins were expressed at levels comparable to wild-type (Western blot in Figure 4D), but both showed a 3- to 5-fold decrease in fold of activation as compared with the wild-type. Furthermore, the absolute magnitude of activation by the P625A mutant is only 5% of wild-type. The results with the P625A mutant are consistent with a previous study where the analogous rat GR mutant (P643A) was also defective in transactivation (Caamano et al., 1998). Together, these results establish that residues comprising the dimer interface are important for the GR transactivation function.

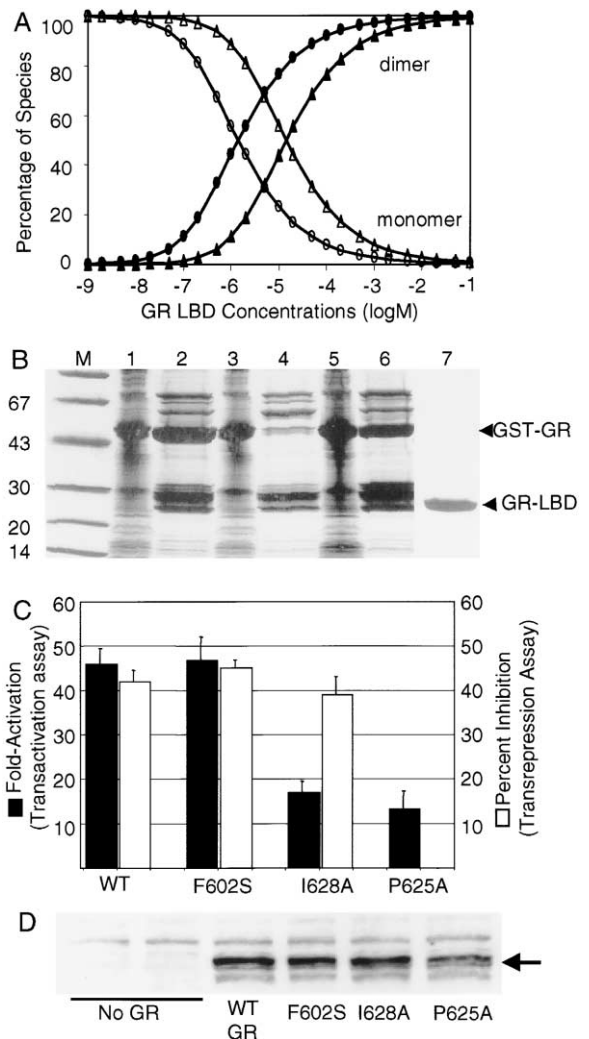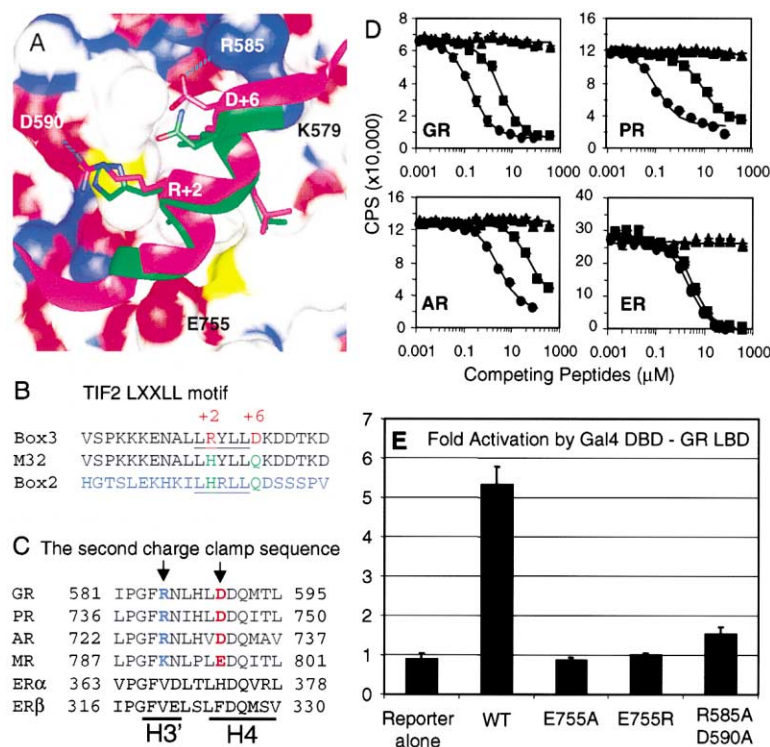We also tested the ability of the GR mutants to inhibit

Figure 4. Functional roles of the GR Dimer Interface

(A) Dimer-monomer distributions of the F602S GR LBD (circles) and the I628A/F602S LBD (triangles) as analyzed by analytic ultra-centrifugation.

(B) Comparison of the protein solubility of the P625A/F602S mutant (lanes 3–4) and the I628A/F602S mutant (lanes 5–6) with the F602S mutant (lanes 1–2). Lanes 1, 3, and 5 represent pellet fractions and lanes 2, 4, and 6 represent soluble fractions. The purified I628A/F602S mutant LBD is shown in lane 7 with molecular weight markers indicated (lane M in Kd).

(C) Transactivation and transrepression by the wild-type and mutant GRs, where the I628A and P625A mutations are made in the dimer interface. The EC50 of dexamethasone for wild-type, F602S, I628A, and P625A receptors is 26, 28, 400, and >2000 nM, respectively. The full level of activation by the P625A mutant is only 5% of wild-type.

(D) Western blots showing the expression of GR.

activation by NF-κB. In this assay, we used a reporter driven by the promoter from the monocyte chemoattractant protein-1 (MCP-1), which is a well-characterized NF-κB activated gene (Ping et al., 1999). In contrast to the transactivation assay, GR with the I628A mutation repressed the MCP-1 promoter activity to the same extent as the wild-type or the F602S receptor (Figure 4C). However, the P625A mutant was inactive in this assay. This defect in activity of the P625A mutant in both assays is consistent with previous studies that indicated that

Figure 5. Structural Basis for the Specificity of Coactivator Motifs

(A) A superposition of the TIF2 third motif (purple) with the SRC-1 motif (green) on the surface of the GR coactivator binding site, where color is based on atom types (carbons: white, sulfur: yellow, nitrogen: blue and oxygen: red). The hydrogen bonds between the TIF2 residues (R+2 and D+6) and the GR residues (D590 and R585) that form the second charge clamp are indicated by green dashed lines.

(B) Sequences of the second and third coactivator motifs in TIF2, and the mutated peptide M32, where the charged residues R+2 and D+6 in the third motif have been replaced with the corresponding residues from the second motif, H+2 and Q+6.

(C) Conservation of amino acids in the second charge clamp. Sequence alignment of GR, AR, PR, and MR with arrows indicating the residues that form the second charge clamp.

(D) Effects of the R+2H and D+6Q mutation (the M32 peptide) on the binding of the coactivator motifs to GR, PR, AR, and ERβ. Dose inhibition curves are shown for the binding of the TIF2 third motif (circles) and the mutated third motif (squares) with control curves of DMSO (triangles). Compared with the wild-type TIF2 third motif, the mutated motif decreases its affinity to GR, AR, and PR by 15- to 50-fold, but has little effect (<2-fold) on binding to ERβ.

(E) Effects of the second charge clamp mutations (R585A and D590A) on the activation mediated by the GR LBD, as compared with the wild-type GR LBD or the mutations in the first charge clamp from the AF-2 helix (E755A or E755R).

Recognition of the TIF2 LXXLL Motif

Coactivators such as SRC-1 and TIF2 contain three LXXLL motifs, and all previous crystal structures of LBD/coactivator complexes were solved with the first or the second LXXLL motif. The GR LBD/TIF2 complex is the first structure with the third LXXLL motif, and it provides an unexpected explanation for the preferential binding of this motif to the receptor (Ding et al., 1998). In the GR LBD structure, the LLRYLL sequence in the TIF2 motif forms a two-turn α helix that orients the hydrophobic leucine side chains into a groove formed in part by the AF-2 helix and residues from helices 3, 3′, 4 , and 5 (Figure 2). The N- and C-terminal ends of the coactivator helix are clamped by E755 from the AF-2 helix and K579 in helix 3, respectively. The docking mode of the TIF2 LXXLL motif is similar to that seen in the coactivator complexes of RXR, ER, TR, PPARα, and PPARγ (Darimont et al., 1998; Gampe et al., 2000; Nolte et al., 1998; Shiau et al., 1998; Xu et al., 2001). However, unexpectedly, the GR residues D590 and R585 form a second charge clamp that interacts with residues R+2 and D+6 (Figure 5A), which are only present in the third LXXLL motif of coactivators (Figure 5B).

We addressed the functional role of the hydrogen bonds between the second GR charge clamp and the TIF2 coactivator by mutating the residues at the +2 and +6 positions of the third LXXLL motif. Replacing these two residues in the third motif with corresponding residues from the second motif decreased binding to GR (Figure 5D). Therefore, the hydrogen bonds formed with the second charge clamp contribute to the selective binding of the third TIF2 LXXLL motif. We also directly addressed the role of the second charge clamp by mutating the two charged residues D590 and R585 to alanine within the context of a GAL4-GR LBD chimeric receptor. The fusion protein of the wild-type GR LBD with the GAL4-DBD induced 5-fold activation of the reporter driven by the GAL4 DNA binding sites (Figure 5E). Mutations either in the first charge clamp (E755 on the AF-2 helix) or the second charge clamp (residues R585 and D590) dramatically reduced the activation mediated by the GR LBD, demonstrating that both charge clamps are critical for transactivation in vivo.

The residues (D590 and R585) comprising the second charge clamp in GR are conserved in PR and AR but not in ER (Figure 5C). Mutations in the third TIF2 LXXLL motif that alter the second charge clamp dramatically reduce affinity to AR and PR, similar to the result obtained with GR. These data suggest that the subfamily of oxosteroid receptors may share a common mechanism of coactivator selectivity (Figure 5D). In contrast, these TIF2 mutations have little effect on binding to ER.

Recognition of Dexamethasone

In the crystal structure, dexamethasone is completely enclosed within the bottom half of the GR LBD (Figure

the analogous rat mutation (P643A) did not translocate properly to the nucleus in the presence of ligand (Ca-amano et al., 1998). Importantly, the contrasting effects of I628A on transactivation versus transrepression suggest that the monomer and dimer forms of GR may regulate distinct signaling pathways.
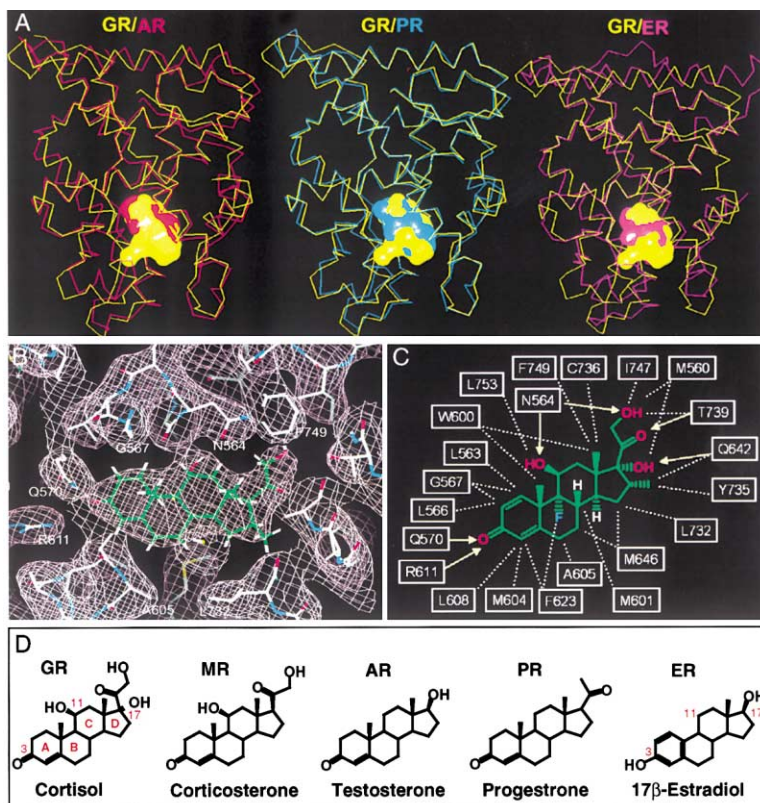
Figure 6. Molecular Basis of Ligand Recognition by GR

(A) Ligand binding pocket of GR and its comparison with the pockets of AR, PR, and ER. GR is colored in yellow in all three overlays.
(B) Electron density map showing dexamethasone and the surrounding residues in GR. The map is calculated with 2Fo-Fc coefficiency and is contoured at one σ.
(C) Schematic representation of GR/dexamethasone interactions. Hydrogen bonds and hydrophobic interactions are indicated by solid arrows and dashed lines, respectively. A possible weak hydrogen bond between C736 and the C20 ketone is omitted for clarity.
(D) Chemical structures of the endogenous steroid hormones and the numbering of the rings and key atoms.

2B). The ligand binding pocket is composed of residues from helices 3, 4, 5, 6, 7, 10, and the AF-2 helix as well as residues from the β strands 1 and 2. Strikingly, compared with the steroid-shaped pocket found in the PR, AR, or ER structures, the GR pocket has an additional branch extending from the center in the side of the steroid pocket. This additional side pocket in GR is formed by the structural rearrangement of helices 6 and 7 (Figure 6A).

The binding mode of dexamethasone can be determined unambiguously by the clear electron density (Figure 6B). The ligand is oriented with its A ring toward the β strands 1 and 2 and its D-ring toward the AF-2 helix. The volume of the GR pocket is approximately 599 Å³ in subunit A and 578 Å³ in subunit B. Although dexamethasone occupies only 65% of the volume, the high affinity binding of dexamethasone to GR is readily explained by the extensive hydrophobic and hydrophilic interactions between the ligand and the protein (Figure 6C). One or more hydrophobic residues within the GR protein contact nearly every atom of the steroid core of dexamethasone.

In addition, all of the hydrophilic groups of dexamethasone form hydrogen bonds with the protein. As shown in Figure 6C, the A ring carbonyl forms direct hydrogen bonds to the guanidinium of R611 and to the γ-amide of Q570. The side chain of N564 is oriented in a way to allow it to make hydrogen bonds to the C ring 11-hydroxyl and 24-hydroxyl. Furthermore, the 21-hydroxyl (off the C17 position) and the 22-carbonyl form hydrogen bonds with residues Q642 and T739, respectively. The extensive hydrogen bond network between GR and the ligand

observed here are likely to contribute to the high affinity binding of dexamethasone.

Interestingly, dexamethasone also makes direct contacts with the AF-2 helix (L753) and the loop preceding the AF-2 helix (residues I747 and F749). These interactions are likely to stabilize the AF-2 helix in the active conformation, and may serve as a molecular basis for ligand-dependent activation of GR.

Discussion

A longstanding problem for GR structural studies has been the expression and purification of an active protein. Here, we have overcome this problem by using a single point mutation, F602S, in the GR LBD. This single mutation resulted in robust expression of a soluble GR LBD and ultimately allowed us to solve its crystal structure. The structure revealed a novel dimer interface, a unique steroid binding pocket, and a second charge clamp responsible for sequence specific binding of a coactivator protein. These structural observations provide critical insights into the protein-ligand and protein-protein interactions that control the GR signaling pathways.

Important Role of the GR Dimer
The GR LBD in the crystal is packed as a symmetric dimer, which is consistent with biochemical data showing that the GR LBD can form a homodimer or a heterodimer with the closely related MR LBD. These earlier studies, however, failed to identify the position or the configuration of the GR dimer interface (Savory et al., 2001). The crystallographically observed GR LBD dimer

interface is strikingly different from the helix-10 dimer interface observed in the previous ER homodimer or RXR heterodimer structures. Structure based sequence alignments reveal that RXR and its heterodimer partners have a consensus dimerization motif of ϕ AK$\phi\phi$ ϕK$\phi\phi$ X ϕR$\phi\phi$ that forms a coiled-coil structure in the first half of H10 (Gampe et al., 2000). ER and HNF4 have the same ϕX$\phi\phi$ repeats that allow them to form homodimers but lack the basic residues in the X position required for heterodimerization. However, GR and its related receptors, PR and AR, have a sequence of F YQLT KLLD S MHEV in the corresponding H10 region that is not able to form a coiled-coil structure due to the deviation of the underlined residues from the ϕX$\phi\phi$ repeats. Furthermore, in the GR structure, the extended C-terminal strand packs against the N terminus of H10 and would further block the dimer configuration seen in the ER and RXR structures (Figure 2B). The difference in the dimer interface between GR and ER may support the evolutionary divergence of ER from the oxosteroid nuclear receptors (Escriva et al., 2000).

We have also confirmed the functional significance of the GR dimer interface by mutagenesis studies. Mutations in the two interface residues P625 and I628 compromise the GR transactivation function, but show different phenotypes in transrepression. While the P625A GR is completely inactive in repression, the I628A mutant is as competent as the wild-type receptor. Using the purified I628A mutant protein, we have confirmed that this mutation decreases the LBD-LBD dimerization affinity. The phenotype of the I628A mutant is similar to that observed with the mouse GR^{dim} mutant, which shows that a defect in DBD dimerization results in loss of GR activation function without affecting transrepression activity (Reichardt et al., 1998).

The GR LBD contains multiple functions including ligand binding, chaperone association, nuclear location, transcription regulation, and others. These functions are interconnected and are highly dependent on the integrity of the three-dimensional structure of the LBD. It is possible that the phenotype of the I628A mutant can be attributed to other functions of the LBD in addition to its effect on dimerization. We have found that the I628A mutant LBD requires a 20-fold higher concentration of dexamethasone to achieve full activation as compared to the wild-type receptor (data not shown). However, the I628A mutant is still competent for nuclear localization and transrepression function at the same ligand concentration used for activation of the wild-type receptor. Thus, a mutation in the dimer interface can selectively decrease the potency for transactivation by the GR LBD.

The different phenotypes of the I628A and P625A mutants may be attributed, in part, to the behavior of their proteins. P625 is located in the β-turn between two β strands and is conserved among steroid receptors. It is likely that the P625A mutation disrupts the β-turn, thus reducing the protein stability. Although in vivo, expression of the full-length receptor either with I628A or P625A appears to be similar (Figure 4D), the P625A mutant LBD is much less soluble than the I628A mutant in *E. coli* (Figure 4B). The P625A mutant also shows defects in nuclear translocation upon ligand binding (data not shown). Our results are consistent with a previous study in which the rat GR with the corresponding mutation P643A was defective in transactivation (Caamano et al., 1998). Although the P643A rat GR retained normal ability to bind DNA, it showed decreased stability for heterocomplex formation with hsp90. Since P625 is the central dimerization residue, this would suggest that the GR dimerization interface might overlap the hsp90 binding site.

Compared with the large interface observed in the RXR dimer structures, the GR LBD dimerization interface is much more limited, reflecting its weaker dimerization affinity (Kd $\sim$1.5 μM for GR versus 1$\sim$10 nM for RXR dimers). In the context of the full-length receptor, the low dimerization affinity of the GR LBD can be compensated by an additional interface found in the DNA binding domain and possibly the hinge region preceding the LBD (Savory et al., 2001). Several reports have highlighted the role of residues in the D loop of the DNA binding domain for stabilizing receptor dimers (Luisi et al., 1991; Reichardt et al., 1998). Normal GR functions require integrity of both interfaces as a mutation in the dimer interface in the DNA binding domain also abolishes GR transactivation function (Reichardt et al., 1998). The discovery of the novel dimer interface in the LBD should provide additional ways to address the functional role of GR dimerization by genetic manipulations.

Coactivator Recognition by the Second Charge Clamp

Nuclear receptors recruit coactivators primarily through the core LXXLL motifs. The fact that there are a large number of coactivators and each contains multiple LXXLL motifs poses a question of how specific recruitment of coactivators is achieved by a given nuclear receptor. Our structure reveals that GR uses two charge clamps to define its sequence specific binding to the TIF2 third motif. The first charge clamp is composed of E755 from the AF-2 helix and K579 from helix-3, which cap the backbone amides and carbonyls of the coactivator helix. Both residues that form the first charge clamp are highly conserved across members of the NR superfamily and dictate a common binding mode for all LXXLL motifs. The second charge clamp is composed of R585 and D590, which form hydrogen bonds with the side chains of the residues R+2 and D+6 that are present in the TIF2 third motif but not in its first or second motif. These interactions with the second charge clamp are responsible, in part, for the binding specificity of GR for the TIF2 third motif. Our results are consistent with the observation that the binding specificity of this motif is encompassed within the TIF2 sequence of KENALLRYLLDKDD (Darimont et al., 1998). The residues from the second charge clamp are conserved in the oxosteroid receptors GR, AR, PR, and MR but are not present in ER or RXR-obligate heterodimers, such as PPAR. Thus, the second charge clamp may account for the differential binding of coactivator motifs by many nuclear receptors. Notably, only the second LXXLL motif is required to mediate ER transactivation while PPARγ requires both the first and the second motifs. Since proteins like SRC-1 and TIF2 function as promiscuous coactivators, the existence of three LXXLL motifs within their sequence may allow them to integrate signaling pathways across multiple
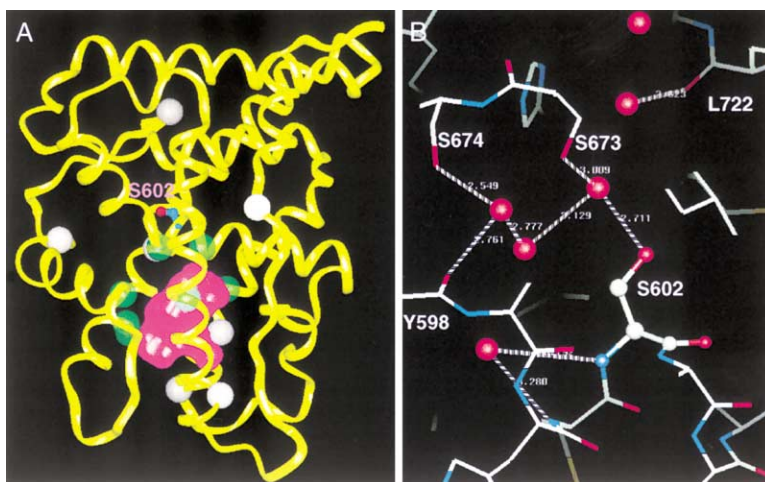
Figure 7. Basis for the GR Mutations

(A) The locations of natural GR mutations are represented as Van der Waals spheres in the overall structure. Green mutations are the residues that contact dexmethasone directly in the structure and the white mutations are in the residues that form the hydrophobic core of the protein. The side chain of S602 is also presented.

(B) Hydrogen bond network mediated by the S602 in the F602S mutant (balls and sticks) and nearby water molecules (red spheres) inside of the protein.

NRs. Alternatively, as yet undiscovered coactivators may exist that modulate GR signal transduction through selective interactions with the second charge clamp.

Hormone Selectivity by Steroid Receptors

Endogenous steroid hormones such as cortisone, testosterone, or progesterone share a similar core chemical structure (Figure 6D) but mediate distinct biological responses. Structural comparisons of GR, AR, PR, and ER have provided insight into how functional specificity is achieved by the steroid receptors. These steroid receptors share over 50% identity in their amino acid sequences and a similar three-dimensional structure. In these structures, the core steroid template (A, B, C, and D rings) assumes a common orientation with the A ring oriented toward the conserved arginine from helix-5 and the D ring toward the AF-2 helix. However, many subtle differences in the secondary structure and the topology of the ligand binding pockets exist in these steroid receptors. In particular, helices 6 and 7 of GR deviate significantly from ER, AR, and PR and produce a unique side pocket in GR (Figure 6A). This pocket may account for the GR selectivity of glucocorticoids, which have larger substituents at the C17α position compared with estrogen, progesterone, and testosterone (Figure 6D). Interestingly, the mineralocorticoids that selectively bind MR have similar substituents at the C17α position. MR may also have a similar pocket for these large C17α substitutes, since the residues that form the GR side pocket are also conserved in MR.

Besides the shape differences, the polar atoms are also distributed differently in the steroid pockets with respect to the specific protein-ligand hydrogen bonds. For example, the polar substituents in steroid hormones are mainly located at positions C3 or C17. In the GR structure, the C3 ketone accepts hydrogen bonds from Q570 and R611, which are also conserved in AR and PR. In ER, the glutamine is replaced by glutamate, which prefers to accept a hydrogen bond from the ligand, therefore accounting for ER's selectivity of a hydroxyl group at the C3 position. These differences in hydrogen bond formation may explain why GR, as well as AR, PR, and MR prefer the steroid hormones with a ketone at the C3 position, whereas ER prefers a hydroxyl group.

The selectivity of GR ligands with larger substituents at the C17 position can be best explained by the larger GR-side pocket. However, as discussed above, MR presumably has a similar pocket to GR. The selectivity of MR for mineralocorticoids can be attributed to the differences in hydrogen bonding patterns between the receptor and the ligands. In fact, the MR selective steroids, corticosterone, aldosterone, and 11-deoxylcorticosterone, all lack the 17α-hydroxyl group, which forms a specific hydrogen bond with Q642 in the GR structure. At this position, MR has a hydrophobic leucine (L848) that would disfavor the presence of a polar hydroxyl in this region. Together, the steroid selectivity appears to be achieved by the complementarity of shape and hydrogen bonding between ligands and the ligand binding pockets in the receptors

Naturally Occurring Mutations in the GR LBD

Missense mutations in the GR LBD have been associated with a number of diseases, such as Cushing's syndrome, autoimmune diseases, and various cancers, and the impact of these mutations can readily be explained by our structure. Based on the location in the GR structure (Figure 7A), these mutations can be classified into two groups. The first group includes the mutations G507C, M601L, M604P, M646T, Y735S, C736S, and L753F. In the structure, these residues are found to make direct contacts with dexamethasone (green balls, Figure 7A), and their mutations most likely result in a GR molecule that is defective in ligand binding. The second group includes mutations of P541A, I559D, C638Y, V729I, Y764N, and F774A (white balls, Figure 7A). In the structure, these residues are involved in hydrophobic interactions within the protein, and their mutations may therefore destabilize the protein. The availability of the GR structure provides an opportunity to determine whether there is any correlation in the locations of these mutations with the clinical phenotypes.

Structural Basis for the Improvement of Protein Solubility by the F602S Mutation

It is intriguing that a single point mutation of F602S has such a dramatic impact on the solubility of the GR LBD. The F602S mutation was one of fourteen mutations that

were suggested by sequence alignment and analysis of a GR homology model. Most of the mutations were targeted for lipophilic residues exposed on the surface of the protein, but had little or no effect on expression or solubility. In contrast, F602 was identified as a buried, lipophilic residue that appeared to fit poorly into its environment within GR. Remarkably, the F602S mutation substantially enhanced the soluble expression of the GR LBD. This result is consistent with the earlier work on the corresponding mutation of the rat GR (F620S), which showed increased receptor activity and was shown to be less dependent on hsp90 proteins for its function (Freeman et al., 2000; Garabedian and Yamamoto, 1992). The GR structure presented here provides a further rationale for the improvement in solubility by the F602S mutation. Although F602 is buried deeply inside of the protein at the first turn of helix-5, where it is sandwiched between helices 3 and 10 (Figure 7A), the hydrophobic side chain of F602 is surrounded by a small hydrophilic cavity (Figure 7B). This hydrophilic cavity is made up of the side chains of S599, S673, S674, and H726, and the backbone carbonyls of residues 598, 599, 670, and 722. The presence of the hydrophobic phenylalanine side chain in the polar environment would be highly unfavorable. This arrangement may cause the local instability that makes the protein prone to aggregation and/or misfolding. The F602S mutation replaces the hydrophobic phenyl ring with a small hydrophilic hydroxyl group, creating a more suitable arrangement within the hydrophilic environment, and apparently overcoming the instability problem. In the crystal structure, the volume created by the F602S mutation is filled by three water molecules. These water molecules not only cap the N terminus of helix-5 but also mediate an extensive hydrogen bond network with the residues that make up the cavity. Interestingly, PR has a serine at the corresponding position, and most of the other nuclear receptors have a glutumate residue at this position. In the structures of other NRs including PPARs, this negatively charged residue forms a pair of hydrogen bonds with a conserved arginine from the loop between helices 8 and 9 (Gampe et al., 2000; Nolte et al., 1998; Xu et al., 1999, 2001). Thus, a hydrophilic residue at position 602 has been evolutionarily conserved in other NRs, possibly to preserve the stability of the protein. GR is the only nuclear receptor with a large hydrophobic residue at this position, and this may account for the difficulty in obtaining a stable protein with wild-type GR constructs.

Extensive studies have indicated that ligand binding of GR in vivo or in vitro depends on the presence of the hsp90 chaperone complex (Pratt and Toft, 1997). It has also been proposed that hsp90 is required for opening the GR ligand binding pocket to allow ligand association (Morishima et al., 2000). Interestingly, using our purified protein, the F602S mutant GR LBD is freely accessible to agonist and antagonist as demonstrated by the competition experiment (Figures 1B and 1C). In the structure, the GR pocket is completely enclosed when it is bound with dexamethasone. Exchange of dexamethasone with RU486 in the purified protein must involve opening the pocket even in the absence of hsp90. However, the in vivo high-affinity binding of ligands still requires the chaperone activity of hsp90 (Bresnick et al., 1989; Picard et al., 1990). It is possible that the rate of ligand binding and/or exchange in vivo is dependent on hsp90. Moreover, the hsp90 complex may also function to prevent the wild-type GR protein from aggregating in vivo by maintaining the structural integrity of the otherwise unstable protein.

Experimental Procedures

Protein Preparation

The GR LBD (residues 521–777), containing a single F602S mutation, was expressed in the presence of 10 μM dexamethasone as a 6 × His-GST fusion protein from the expression vector pET24a (Novagen). The modified fusion protein contains a His-TAG (MKKGHHHHHHG) at the N terminus and a thrombin protease site between GST and the GR LBD. The GR LBD was purified to homogeneity using similar procedures previously described for AR and PR (Matias et al., 2000; Williams and Sigler, 1998). A typical yield of the purified protein is about 1 mg from each liter of cells. To prepare the protein-ligand-coactivator complex, we added a 2-fold excess of the TIF2 peptide to the purified GR LBD, which was present with 50 μM dexamethasone. The ternary complex was then diluted 10-fold with a buffer containing 500 mM ammonium acetate, 50 mM Tris, (pH 8.0), 10% glycerol, 10 mM dithiothreitol, 0.5 mM EDTA, and 0.05% β-n-octoglucoside, and concentrated to 6.3 mg/ml for crystallization. The I628A/F602 mutant LBD was expressed and purified with the same procedures for the F602S mutant LBD except the TIF2 peptide was added during purification.

Crystallization and Data Collection

The GR/dexamethasone/TIF2 crystals were grown at room temperature in hanging drops containing 3.0 μl of the above protein-ligand solutions, and 0.5 μl of well buffer containing 50mM HEPES, (pH 8.0), and 2.0 M ammonium formate. Crystals appeared overnight and continued to grow to a size up to 300 micron within a week. Before data collection, crystals were transiently mixed with the well buffer containing additional 25% of glycerol, and were then flash frozen in liquid nitrogen.

The GR/TIF2/dexamethasone crystals formed in the P6₁ space group, with a = b = 126.014 Å, c = 86.312 Å, α = β =90°, and γ =120°. Each asymmetry unit contains two GR LBDs with 56% of solvent content. The 2.8 Å data set was collected with an in-house Rigaku Raxis IV detector and the 2.5 Å data set was collected with a MAR CCD detector at 17-ID in the facilities of the Industrial Macromolecular Crystallography Association (IMCA) at the Advanced Photon Source. The observed reflections were reduced, merged, and scaled with DENZO and SCALEPACK in the HKL2000 package (Otwinowski and Minor, 1997).

Structure Determination and Refinement

The 2.8 Å structure of the GR/dexamethasone/TIF2 complex was determined by molecular replacement with the AmoRe program (Navaza et al., 1992; Williams and Sigler, 1998; Xu et al., 2001). The initial GR model, containing residues 527–776 of wild-type GR and residues 740–752 of TIF2, was built with the MVP program by combining the PR LBD structure (Williams and Sigler, 1998) with the SRC-1 portion of the PPARα/SRC-1 structure (Navaza et al., 1992; Williams and Sigler, 1998; Xu et al., 2001). Two solutions were obtained from the molecular replacement search with a correlation coefficient of 43% and an R-factor of 45.3%, consistent with two complexes within each asymmetry unit. The phases from the molecular replacement solution were extensively refined with solvent flattening, histogram matching, and 2-fold noncrystallographic symmetry (NCS) averaging as implemented in the CCP4 dm program and produced a clear map for the GR LBD, the TIF2 peptide, and the dexamethasone. Multiple cycles of manual model building, including conversion of side-chains from the SRC-1 and wild-type GR sequences to the actual TIF2 and GR F602S sequences, respectively, was carried out with QUANTA (Accelrys Inc). Structure refinements proceeded with CNX (Brunger et al., 1998), using the maximum likelihood target and NCS constraints, which was relaxed in the final stages of refinement. The 2.5 Å structure of the GR/dexamethasone/TIF2 complex was then determined by using the 2.8 Å structure

as the model. The statistics of the structures and data sets are summarized in Table 1. The 2-fold symmetry axis of the GR dimer was calculated as axis of the rotation that would superimpose one LBD onto the other. The superposition was carried out using the Cα atoms from residues 530–777 of GR. Solvent accessible surface areas were calculated with the Connolly MS program and the MVP program (Connolly, 1983; Lambert, 1997). The pocket volume and binding site accessible waters were calculated with MVP.

Binding Assays
The ligand binding activity of the purified GR LBD was determined by a fluorescence polarization assay. Experiments were conducted by combining 10 nM fluorescence-dexamethasone (Molecular Probes) with increasing concentrations of the purified GR LBD in a buffer containing 10 mM HEPES (pH 7.4), 0.15 M NaCl, 3 mM EDTA, 0.005% polysorbate-20 and 5 mM DTT. The fluorescence polarization values for each concentration of receptor were determined using a BMG PolarStar Galaxy fluorescence plate reader with 485 nm excitation and 520 nm emission filters. The apparent Kd values were determined with a nonlinear least squares fit of the data for a simple 1:1 interaction. Note that the apparent affinity for the binding of the fluorescent dexamethasone (60 nM) is slightly weaker than previously reported values most likely due to the presence of unlabeled dexamethasone that remains in the protein preparations despite extensive dialysis.

The binding of the TIF2 coactivator motif to the GR LBD was determined by surface plasmon resonance using a Biacore 3000 instrument. Experiments were conducted at 25°C with ~500 RU biotinylated TIF2 peptide bound onto a streptavidin chip. Running buffer (10 mM HEPES [pH 7.4], 150 mM NaCl, 3 mM EDTA, 0.005% polysorbate-20, and 5 mM DTT) was used with a flow rate of 5 μl/ min. Binding signals were determined by injecting varied concentrations of the GST-GR LBD (F602S) with no added ligand, 5-fold molar excess of dexamethasone, or RU486. A dose-response curve was constructed using the equilibrium response taken 10 s before the end of the association phase minus the response from a flow cell with no immobilized peptide.

The effects of the R+2H and D+6Q mutations in the TIF2 third motif on the binding to GR, PR, AR, and ERβ were determined by chemical mediated energy transfer assays using the AlphaScreen Technology from Packard BioScience, as described recently for nuclear receptors (Xu et al., 2002). Proteins were prepared by expressing the AR LBD (residues 662–919), the PR LBD (residues 678–933), and the GR LBD (residues 521–777 with F602S) as 6 × His-GST fusion proteins in the presence of the respective ligands R1881, progesterone, and dexamethasone. The ERβ LBD (residues 257–530) was prepared in the absence of ligand. These proteins were partially purified by Ni 2+ chromatography. The experiments were conducted with approximately 2 nM receptor LBD, 4 nM of biotinylated peptide containing the TIF2 third motif in a buffer containing 50 mM MOPS (pH 7.4), 50 mM NaF, 0.05 mM CHAPS, 0.1 mg/ml bovine serum albumin, and 5 mM dithiothreitol. An excess amount of 1 μM R1881, progesterone and dexamethasone, and estradiol was added to AR, PR, GR, and ERβ, respectively. An AlphaScreen hexahistidine detection kit was utilized and the donor and acceptor bead concentrations were 8 μg/ml. The binding signals were obtained with increasing concentrations of the unlabeled third motif peptide or the mutated peptide and detected using a Packard BioScience AlphaQuest HTS. The IC50 values were constructed from a nonlinear least squares fit of the data for a simple 1:1 interaction and are an average of four repeated experiments with DMSO as controls.

In Vitro Dimerization Assays
The solution state of the GR LBD was determined by dynamic light scattering (Protein Solution Inc) or by analytical ultra-centrifugation using a Beckman (Fullerton, CA) XL-I centrifuge. In ultra-centrifugation, 100 μl of each sample was centrifuged against 110 μl of the equivalent buffer blank using a six-sector charcoal-filled epon centerpiece in an An-60 Ti rotor. Solvent density [100 mM sodium phosphate (pH 8), and 500 mM sodium chloride] was determined empirically to be 1.035 at 4°C using a Mettler (Highstown, NJ) DA-110 density /specific gravity meter calibrated against water. The partial

specific volume of the protein, $\bar{v}$, was calculated as described (Cohn and Edsall, 1943). Adjustments for temperature were made using the appropriate equation that has been modified to use $\bar{v}$ values derived for each amino acid at 25°C (Durchschlag, 1986). The partial specific volume of GR LBD was calculated to be 0.736 mL/g at 4°C. Runs were performed at 17,500, 20,000, 22,500, and 25,000 rpm at 4°C. Data sets were obtained as radial distance versus absorbance. Scans were taken at 280 nm at 1 hr intervals throughout the run. Sedimentation equilibrium was judged by the absence of change between plots of several successive scans after approximately 20–30 hr at each speed. The raw data (from the meniscus to the back of the cell) was analyzed by an adaptation of the Beckman/ Microcal Origin nonlinear regression software package using multiple iterations of the Marquardt-Levenberg algorithm for parameter estimation. Multiple models were employed to determine the most accurate description of the macromolecular species.

Functional Assays of the GR Dimer Interface
Assessment of the functional activity of full-length, wild-type, and mutant GR constructs was carried out using the transient transfection assay. To assess transactivation, expression vector (pRS vector) encoding full-length, wild-type, or mutated GR protein (0.1 ng) was cotransfected into CV-1 cells with a reporter plasmid (15 ng) containing luciferase under transcriptional control of the GR-responsive region in the MMTV promoter (List et al., 1999). To assess transrepression, GR expression vectors (5 ng) were cotransfected with pCMV-4T expression vector (0.1 ng) encoding p65 NF-κB subunit, and a reporter plasmid (10 ng) containing a fragment of the NF-κB-responsive MCP-1 promoter (Ping et al., 1999). CV-1 cells were transiently transfected with lipofectamine (Invitrogen, Inc.) as described (Moore et al., 2000; Willson et al., 1996). Cells were treated with 100 nM dexamethasone on day 2 of the transfection procedure and reporter activity assessed at day 3. Luciferase activity was normalized using an internal constitutively active reporter to control for well-to-well variation. Data were plotted as fold activation by dexamethasone after subtracting background activity of CV-1 cells transfected in the absence of added receptor.

In Vivo Assays of the Second Charge Clamp Mutations
The effect of the primary and secondary charge clamp mutations on activation in vivo was determined using a Gal4 transactivation assay. The wild-type GR LBD (486–777) or mutated GR LBD was fused in frame with the Gal4 DBD in a mammalian expression vector (pSG5). The Gal4 DBD-GR LBD fusion vector (8 ng) was cotransfected into CV-1 cells with a reporter plasmid pUAS-TK (8 ng) containing luciferase under transcriptional control of the Gal4-responsive region. CV-1 cells were transiently transfected as previously described with the exception of Fugene 6 (Roche) as the transfection reagent.

Western Blotting
Equal amounts of total cellular protein were electrophoresed on 12% SDS-PAGE and transferred to Trans-Blot nitrocellulose membranes (BioRad, Hercules, CA). GR was visualized using an ECL detection system (Amersham Pharmacia Biotech, Piscataway, NY) after incubation with rabbit polyclonal antibody (anti-human GR, sc-1002 Santa Cruz Biotechnology, Santa Cruz, CA) and a horseradish peroxidase-linked goat anti-mouse secondary antibody (Southern Biotech Associates, Birmingham, AL).

References

Barnes, P.J., Pedersen, S., and Busse, W.W. (1998). Efficacy and safety of inhaled corticosteroids. New developments. Am. J. Respir. Crit. Care Med. *157*, S1–53.

Bourguet, W., Ruff, M., Chambon, P., Gronemeyer, H., and Moras, D. (1995). Crystal structure of the ligand-binding domain of the human nuclear receptor RXR-α. Nature *375*, 377–382.

Bresnick, E.H., Dalman, F.C., Sanchez, E.R., and Pratt, W.B. (1989). Evidence that the 90-kDa heat shock protein is necessary for the steroid binding conformation of the L cell glucocorticoid receptor. J. Biol. Chem. *264*, 4992–4997.

Brunger, A.T., Adams, P.D., Clore, G.M., DeLano, W.L., Gros, P., Grosse-Kunstleve, R.W., Jiang, J.S., Kuszewski, J., Nilges, M., Pannu, N.S., et al. (1998). Crystallography & NMR system: a new software suite for macromolecular structure determination. Acta Crystallogr. D Biol. Crystallogr. *54*, 905–921.

Brzozowski, A.M., Pike, A.C., Dauter, Z., Hubbard, R.E., Bonn, T., Engstrom, O., Ohman, L., Greene, G.L., Gustafsson, J.A., and Carlquist, M. (1997). Molecular basis of agonism and antagonism in the oestrogen receptor. Nature *389*, 753–758.

Caamano, C.A., Morano, M.I., Dalman, F.C., Pratt, W.B., and Akil, H. (1998). A conserved proline in the hsp90 binding region of the glucocorticoid receptor is required for hsp90 heterocomplex stabilization and receptor signaling. J. Biol. Chem. *273*, 20473–20480.

Chen, J.D., and Evans, R.M. (1995). A transcriptional co-repressor that interacts with nuclear hormone receptors. Nature *377*, 454–457.

Cohn, E.J., and Edsall, J.T. (1943). Proteins, Amino Acids and Peptides as Ions and Dipolar Ions (New York: Rheinhold).

NRNC (Nuclear Receptors Nomenclature Committee). (1999). A unified nomenclature system for the nuclear receptor superfamily. Cell *97*, 161–163.

Connolly, M.L. (1983). Solvent-accessible surfaces of proteins and nucleic acids. Science *221*, 709–713.

Darimont, B.D., Wagner, R.L., Apriletti, J.W., Stallcup, M.R., Kushner, P.J., Baxter, J.D., Fletterick, R.J., and Yamamoto, K.R. (1998). Structure and specificity of nuclear receptor-coactivator interactions. Genes Dev. *12*, 3343–3356.

Ding, X.F., Anderson, C.M., Ma, H., Hong, H., Uht, R.M., Kushner, P.J., and Stallcup, M.R. (1998). Nuclear receptor-binding sites of coactivators glucocorticoid receptor interacting protein 1 (GRIP1) and steroid receptor coactivator 1 (SRC-1): multiple motifs with different binding specificities. Mol. Endocrinol. *12*, 302–313.

Durchschlag, H. (1986). Specific volumes of biological macromolecules and some other molecules of interest. In Thermodynamic Data for Biochemistry and Biotechnology, H.J. Hinz, ed. (New York: Springer-Verlag), pp. 45–128.

Escriva, H., Delaunay, F., and Laudet, V. (2000). Ligand binding and nuclear receptor evolution. Bioessays *22*, 717–727.

Freeman, B.C., Felts, S.J., Toft, D.O., and Yamamoto, K.R. (2000). The p23 molecular chaperones act at a late step in intracellular receptor action to differentially affect ligand efficacies. Genes Dev. *14*, 422–434.

Gampe, R.T., Jr., Montana, V.G., Lambert, M.H., Miller, A.B., Bledsoe, R.K., Milburn, M.V., Kliewer, S.A., Willson, T.M., and Xu, H.E. (2000). Asymmetry in the PPARγ/RXRα crystal structure reveals the molecular basis of heterodimerization among nuclear receptors. Mol. Cell *5*, 545–555.

Garabedian, M.J., and Yamamoto, K.R. (1992). Genetic dissection of the signaling domain of a mammalian steroid receptor in yeast. Mol. Biol. Cell *3*, 1245–1257.

Heery, D.M., Kalkhoven, E., Hoare, S., and Parker, M.G. (1997). A signature motif in transcriptional co-activators mediates binding to nuclear receptors. Nature *387*, 733–736.

Horlein, A.J., Naar, A.M., Heinzel, T., Torchia, J., Gloss, B., Kurokawa, R., Ryan, A., Kamei, Y., Soderstrom, M., Glass, C.K., et al. (1995). Ligand-independent repression by the thyroid hormone receptor mediated by a nuclear receptor co-repressor. Nature *377*, 397–404.

Lambert, M.H. (1997). Docking conformationally flexible molecules into protein binding sites. In Practical Application of Computer-Aided Drug Design, P.S. Charifson, ed. (New York, NY: Marcel-Dekker), pp. 243–303.

Le Douarin, B., Nielsen, A.L., Garnier, J.M., Ichinose, H., Jeanmougin, F., Losson, R., and Chambon, P. (1996). A possible involvement of TIF1 α and TIF1 β in the epigenetic control of transcription by nuclear receptors. EMBO J. *15*, 6701–6715.

List, H.J., Lozano, C., Lu, J., Danielsen, M., Wellstein, A., and Riegel, A.T. (1999). Comparison of chromatin remodeling and transcriptional activation of the mouse mammary tumor virus promoter by the androgen and glucocorticoid receptor. Exp. Cell Res. *250*, 414–422.

Luisi, B.F., Xu, W.X., Otwinowski, Z., Freedman, L.P., Yamamoto, K.R., and Sigler, P.B. (1991). Crystallographic analysis of the interaction of the glucocorticoid receptor with DNA. Nature *352*, 497–505.

Matias, P.M., Donner, P., Coelho, R., Thomaz, M., Peixoto, C., Macedo, S., Otto, N., Joschko, S., Scholz, P., Wegg, A., et al. (2000). Structural evidence for ligand specificity in the binding domain of the human androgen receptor. Implications for pathogenic gene mutations. J. Biol. Chem. *275*, 26164–26171.

McKay, L.I., and Cidlowski, J.A. (1999). Molecular control of immune/inflammatory responses: interactions between nuclear factor-κ B and steroid receptor-signaling pathways. Endocr. Rev. *20*, 435–459.

Moore, L.B., Parks, D.J., Jones, S.A., Bledsoe, R.K., Consler, T.G., Stimmel, J.B., Goodwin, B., Liddle, C., Blanchard, S.G., Willson, T.M., et al. (2000). Orphan nuclear receptors constitutive androstane receptor and pregnane X receptor share xenobiotic and steroid ligands. J. Biol. Chem. *275*, 15122–15127.

Morishima, Y., Murphy, P.J., Li, D.P., Sanchez, E.R., and Pratt, W.B. (2000). Stepwise assembly of a glucocorticoid receptor hsp90 heterocomplex resolves two sequential ATP-dependent events involving first hsp70 and then hsp90 in opening of the steroid binding pocket. J. Biol. Chem. *275*, 18054–18060.

Navaza, J., Gover, S., and Wolf, W. (1992). AMoRe: a new package for molecular replacement. In Molecular Replacement: Proceedings of the CCP4 Study Weekend, E.J. Dodson, ed. (Daresbury, UK: SERC), pp. 87–90.

Nolte, R.T., Wisely, G.B., Westin, S., Cobb, J.E., Lambert, M.H., Kurokawa, R., Rosenfeld, M.G., Willson, T.M., Glass, C.K., and Milburn, M.V. (1998). Ligand binding and co-activator assembly of the peroxisome proliferator-activated receptor-γ. Nature *395*, 137–143.

Onate, S.A., Tsai, S.Y., Tsai, M.J., and O'Malley, B.W. (1995). Sequence and characterization of a coactivator for the steroid hormone receptor superfamily. Science *270*, 1354–1357.

Otwinowski, Z., and Minor, W. (1997). Processing of x-ray diffraction data collected in oscillation mode. In Macromolecular Crystallography, J.C.W. Carter, and R. M. Sweet, eds. (New York, NY: Academic Press), pp. 307–326.

Picard, D., Khursheed, B., Garabedian, M.J., Fortin, M.G., Lindquist, S., and Yamamoto, K.R. (1990). Reduced levels of hsp90 compromise steroid receptor action in vivo. Nature *348*, 166–168.

Ping, D., Boekhoudt, G.H., Rogers, E.M., and Boss, J.M. (1999). Nuclear factor-κ B p65 mediates the assembly and activation of the TNF-responsive element of the murine monocyte chemoattractant-1 gene. J. Immunol. *162*, 727–734.

Pratt, W.B., and Toft, D.O. (1997). Steroid receptor interactions with heat shock protein and immunophilin chaperones. Endocr. Rev. *18*, 306–360.

Reichardt, H.M., Kaestner, K.H., Tuckermann, J., Kretz, O., Wessely, O., Bock, R., Gass, P., Schmid, W., Herrlich, P., Angel, P., and Schutz, G. (1998). DNA binding of the glucocorticoid receptor is not essential for survival. Cell *93*, 531–541.

Reichardt, H.M., Tronche, F., Berger, S., Kellendonk, C., and Schutz, G. (2000). New insights into glucocorticoid and mineralocorticoid signaling: lessons from gene targeting. Adv. Pharmacol. *47*, 1–21.

Renaud, J.P., Rochel, N., Ruff, M., Vivat, V., Chambon, P., Gronemeyer, H., and Moras, D. (1995). Crystal structure of the RAR-γ ligand-binding domain bound to all-trans retinoic acid. Nature *378*, 681–689.

Sack, J.S., Kish, K.F., Wang, C., Attar, R.M., Kiefer, S.E., An, Y., Wu, G.Y., Scheffler, J.E., Salvati, M.E., Krystek, S.R., Jr., et al. (2001). Crystallographic structures of the ligand-binding domains of the androgen receptor and its T877A mutant complexed with the natural agonist dihydrotestosterone. Proc. Natl. Acad. Sci. USA *98*, 4904–4909.

Savory, J.G., Prefontaine, G.G., Lamprecht, C., Liao, M., Walther, R.F., Lefebvre, Y.A., and Hache, R.J. (2001). Glucocorticoid receptor homodimers and glucocorticoid-mineralocorticoid receptor hetero-dimers form in the cytoplasm through alternative dimerization inter-faces. Mol. Cell. Biol. *21*, 781–793.

Shiau, A.K., Barstad, D., Loria, P.M., Cheng, L., Kushner, P.J., Agard, D.A., and Greene, G.L. (1998). The structural basis of estrogen recep-tor/coactivator recognition and the antagonism of this interaction by tamoxifen. Cell *95*, 927–937.

Valentine, J.E., Kalkhoven, E., White, R., Hoare, S., and Parker, M.G. (2000). Mutations in the estrogen receptor ligand binding domain discriminate between hormone-dependent transactivation and transrepression. J. Biol. Chem. *275*, 25322–25329.

Voegel, J.J., Heine, M.J., Zechel, C., Chambon, P., and Gronemeyer, H. (1996). TIF2, a 160 kDa transcriptional mediator for the ligand-dependent activation function AF-2 of nuclear receptors. EMBO J. *15*, 3667–3675.

Voegel, J.J., Heine, M.J., Tini, M., Vivat, V., Chambon, P., and Grone-meyer, H. (1998). The coactivator TIF2 contains three nuclear recep-tor-binding motifs and mediates transactivation through CBP bind-ing-dependent and -independent pathways. EMBO J. *17*, 507–519.

Wagner, R.L., Apriletti, J.W., McGrath, M.E., West, B.L., Baxter, J.D., and Fletterick, R.J. (1995). A structural role for hormone in the thyroid hormone receptor. Nature *378*, 690–697.

Werner, S., and Bronnegard, M. (1996). Molecular basis of glucocor-ticoid-resistant syndromes. Steroids *61*, 216–221.

Williams, S.P., and Sigler, P.B. (1998). Atomic structure of progester-one complexed with its receptor. Nature *393*, 392–396.

Willson, T.M., Cobb, J.E., Cowan, D.J., Wiethe, R.W., Correa, I.D., Prakash, S.R., Beck, K.D., Moore, L.B., Kliewer, S.A., and Lehmann, J.M. (1996). The structure-activity relationship between peroxisome proliferator-activated receptor γ agonism and the antihyperglycemic activity of thiazolidinediones. J. Med. Chem. *39*, 665–668.

Xu, H.E., Lambert, M.H., Montana, V.G., Parks, D.J., Blanchard, S.G., Brown, P.J., Sternbach, D.D., Lehmann, J.M., Wisely, G.B., Willson, T.M., et al. (1999). Molecular recognition of fatty acids by peroxisome proliferator-activated receptors. Mol. Cell *3*, 397–403.

Xu, H.E., Lambert, M.H., Montana, V.G., Plunket, K.D., Moore, L.B., Collins, J.L., Oplinger, J.A., Kliewer, S.A., Gampe, R.T., Jr., McKee, D.D., et al. (2001). Structural determinants of ligand binding selectiv-ity between the peroxisome proliferator-activated receptors. Proc. Natl. Acad. Sci. USA *98*, 13919–13924.

Xu, H.E., Stanley, T.B., Montana, V.G., Lambert, M.H., Shearer, B.G., Cobb, J.E., McKee, D.D., Galardi, C.M., Plunket, K.D., Nolte, R.T., et al. (2002). Structural basis for antagonist-mediated recruitment of nuclear co-repressors by PPARα. Nature *415*, 813–817.

Zhang, S., Liang, X., and Danielsen, M. (1996). Role of the C terminus of the glucocorticoid receptor in hormone binding and agonist/antagonist discrimination. Mol. Endocrinol. *10*, 24–34.

Accession Numbers

The Protein Data Bank ID code for the structure reported here is 1M2Z.